Structure Development in Amorphous Starch as Revealed by X-ray Scattering: Influence of the Network Structure and Water Content

R. K. Bayer,[1] M. E. Cagiao,[2] F. J. Baltá Calleja[2]

[1]*Universität Gesamthochschule Kassel, Mönchebergstr. 3, D-34125 Kassel, Germany*
[2]*Instituto de Estructura de la Materia, CSIC, Serrano 119, 28006 Madrid, Spain*

ABSTRACT: The evolution of the amorphous structure of starch was characterized during the drying process by real-time X-ray wide-angle scattering. The X-ray diffractograms of injection-molded starch show two superposed, rather broad, scattering maxima indicative of noncrystalline structures. The location of the two peaks has been associated to disordered starch single helices. A third maximum that arises upon drying the material in vacuum is associated to the scattering emerging from regions containing double helices. A model for the starch network is proposed, assuming a primary and a secondary component. The wider, temperature stable component appearing first, is correlated to the entanglement network of the melt. The narrower network component, which is created later, at lower temperature (secondary network), is explained by the formation of double helix regions that densify the wider primary network. The secondary network is increased strongly by the drying process. X-ray experiments performed during the penetration of water, provoking a higher molecular mobility, reveal a better-packed helical structure that becomes the precursor of a double helix crystalline formation. When temperature increases, the secondary network is dissolved and water molecules arrange themselves in better-organized crystals as strongly bound crystal water. © 2005 Wiley Periodicals, Inc. J Appl Polym Sci 99: 1880–1886, 2006

Key words: amorphous starch; structure development; WAXS

INTRODUCTION

Preceding studies show that amorphous starch exhibits a typical halo in the scattering pattern at $2\theta = 19$–$20°$.[1,2] Sometimes two additional maxima superposed at lower scattering angles can also be observed. Müller et al.[3] calculated the wide-angle diffraction profiles for amorphous starch, using a single helix conformation model, and compared the derived profiles with experimental curves for amylose dissolved in water. Previous results show a good agreement between calculated and experimental data for the maxima at $2\theta_{max} = 20°$ and at $12.5°$.[1,2] In other words, from the conformation of a statistical single helix, one obtains an intermolecular distance distribution with two main diffraction peaks. In the case of double helices (composed of two parallel left-handed single helices in B-form as proposed by Imberty[4] in amorphous conformation) Müller calculated a less broader maximum at $2\theta_{max} = 17°$[3] that has not yet been experimentally verified.

According to Gidley,[5] the amylose molecules in dilute solution appear as single helices, showing a statistical conformation. However, for concentrations higher than 0.8%, the molecules build up a network in which the net-points are formed by double helices, giving rise to a sol–gel transition. From the aforementioned studies, one may expect that the structure of both amorphous components should build up a network of flexible single helices connected by double helices.[6] Our own wide angle X-ray scattering experiments (WAXS)-studies suggest, that a pronounced maximum at 17° can be ascribed to a disordered component of double helices, while the maximum at 20° can be explained by the amorphous component of single helices.[7]

The influence of water during the crystallization of amylopectine molecules has been studied by several authors.[8–12] Donald[8,9] investigated the development of a long period near 9 nm using SAXS and the appearance of the (100) B-crystal reflection at $2\theta = 5.5°$ ($d_{100} = 0.16$ nm). In addition, one observes a clear increase of the background scattering below 12°. Del-

mas[10,11] studied the structure development of a paste of amylose powder with 30% water annealed at different temperatures. Her X-ray scattering results show that the onset of crystallization is always accompanied by an excess of continuous scattering at low angles. Müller shows, in addition, that the increase of the background scattering is due to the rise of the electron density difference between the starch molecules and the surrounding water.

Our own results confirm that the crystal structure of potato starch is destroyed after injection molding; however, a new crystalline structure can be developed by means of appropriate water conditioning.[13]

From the observations of Mercier,[12] one finally concludes that the penetration of water into amorphous starch leads to a shift of the main amorphous halo towards higher scattering angles.

In a separate study,[14] two components of the amylose network of different thermal stability were distinguished. According to these studies, a strong modification of the amylose network happens at the transition from 120 to 140°C. Temperature stable net-points are originated directly by fixation of the entanglement network of molten starch below 135°C. The mobile entanglements within the melt are fixed (primary network). Below this temperature thick A- and B- crystals may form from double helices, arising from single helices. From FTIR data of Bernazzani[11] below 75°C, a further densification of the starch network is observed. Crystallization is strongly confined by this densification, as shown by X-ray data from Bernazzani et al.[10] Hence, other authors[15] obtain a decrease of the FTIR band that is responsible for the amylose network, when temperature surpasses 75°C. Gidley[5] mentions two possibilities for the formation of an amylose gel: (a) Formation of net-points from entanglements of single helix molecules and (b) Formation of double helix net-points from two free single helices. Furthermore, Gidley shows that the critical gel concentration of the double helix network is much smaller than the overlap concentration of the entanglement network. This means that for a given mean chain length, the double helix network is much denser than the entanglement network. Accordingly, the densification of the entanglement network below 75°C is apparently due to the connection of single helices into double helices[14] (denser secondary network of double helices that stabilizes the entanglement network built at higher temperatures). In a further publication, we will show that only the primary (AM)-network controls the swelling behavior in water, while the secondary network, which includes AP too, forms the gel obtained after swelling.

According to our previous results,[7] the evaporation of water is much faster at 140°C than at 120°C. It was shown that the evaporation at 140°C takes place in only one step, which means Fickanian behavior. At 120°C, one clearly distinguishes between diffusion of free water (quick) and water strongly bound to the starch molecule (slow). The loss of fixing the entanglement network at 135°C favors the molecular mobility of water within starch.

The aim of the present study is to complement the above investigations to examine the influence of (a) the inner network structure, (b) the water content, and (c) the treatment temperature, on the structural changes occurring in amorphous injection molded starch, as revealed by real-time wide angle X-ray scattering.

EXPERIMENTAL

Materials

Potato starch samples were injection molded (employing an ARBURG-Allrounder 250S) using the elongational-flow injection molding method.[16,17] This method yields ductile oriented amorphous starch materials. A melt temperature of 140°C and a molding temperature of 25°C were used, respectively. The molded samples were kept at ambient atmosphere, i.e., a humidity of 12%, and 1-mm cuts were prepared. The samples were investigated in situ by WAXS diffraction as follows:

1. X-ray experiments were first performed on amorphous air-conditioned samples. The samples were heated up in 150 s at the selected temperature (120 and 140°C, respectively) and maintained at this temperature for approximately 30 min. In situ scattering patterns were recorded during isothermal heating of the samples. Vacuum was applied during the whole experiment.

2. Air conditioned samples were brought into water saturated atmosphere and subjected to stepwise thermal treatment at room temperature, 40, 69, 88, and 94°C, respectively, for periods of 10 min each. For this purpose, sealed glass tubes with a 0.1-mm wall thickness were used. The lower part of the tubes was filled with a small amount of water, while in the upper part the sample was placed, avoiding the contact between the starch and the water surface.

3. Finally, a third set of amorphous samples kept under high humidity was heated up to 97°C, at a heating rate of 5°C/min, with the purpose of studying them in the molten state. Finally, samples were stepwise cooled down.

Techniques

WAXS were performed using a double focusing camera adapted for the synchrotron radiation source at the

polymer beamline A2 of HASYLAB, DESY, Hamburg. The wavelength used was 0.15 nm, with a band pass of $\delta\lambda/\lambda = 5 \times 10^{-5}$. Scattering patterns were recorded every 30 s using a linear position sensitive-detector. The patterns were corrected for fluctuations in intensity of the primary beam and for the background. The accumulation time per frame was 30 s.

RESULTS AND DISCUSSION

### Structural changes of amorphous starch upon drying

At the beginning of the drying process at 140°C in vacuum, one observes two major contributions to the amorphous halo at 16° and 20° (2θ), as illustrated in Figure 1((a). At the end of the drying process at 140°C, one sees a clear increase of the intensity of the first maximum (peak 1) over the second one (peak 2) (Fig. 1(b)).

In fact, one can decompose the amorphous scattering curve into three components. We have used a program that uses Gauss curves in which the height, integral breadth, and the position of the maxima can be independently chosen. The right hand-side of the experimental curve (2nd maximum) is, thus, adjusted to a Gauss curve, having a maximum at approximately 19–20°, associated to the single helices component as pointed out above. The program derives the shape and position of the 1st maximum (middle maximum), associated to the scattering of the double helices, from the rest of the experimental curve. A good separation of both components is feasible as shown in Figure 1. One sees that the position of peak 2 is not influenced by the overlapping of the right hand side of the maximum 1. Consequently, the position and shape of peak 1 can be easily derived. It is noteworthy that the integral breadth of maximum 1 influences notably the overlapping zone of both diffraction maxima in the experimental curve. On the other hand, the overlapping of the two diffraction maxima leaves at small scattering angles an excess scattering from the experimental curve. This scattering can also be adjusted to a Gaussian curve (3rd peak at 12.5°, as mentioned in the Introduction), which is also due to disordered single helices. From the breadth of the peaks 1 and 2, one can conclude that the double helices have a stronger tendency to aggregate than the single helices. One may think of small aggregated regions of double helices connected by loose single helix molecules. This corresponds well to the model of net-points of a starch gel proposed by Gidley.[5]

Figure 2 shows the development of the relative contribution of peak 1 at two different temperatures. The sum of peaks 2 and 3 (not shown here) exhibits just a complementary behavior. Thus, when the area of peak 1 increases the sum of peaks 2 and 3 decreases. This
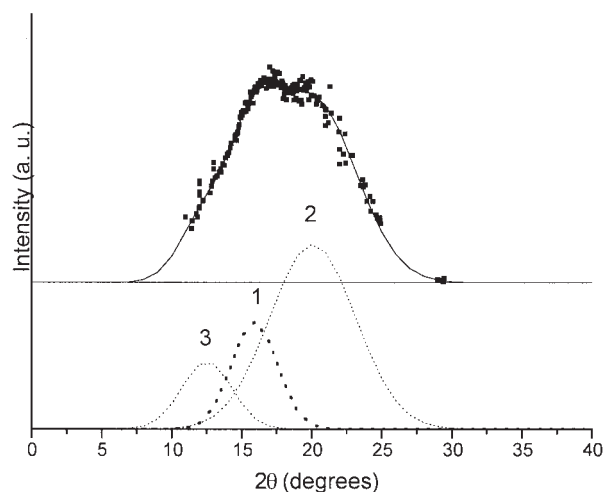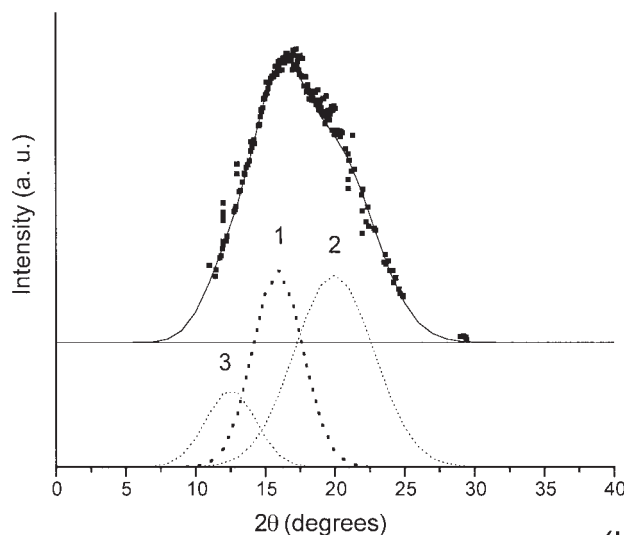

Figure 1 WAXS pattern at the beginning (a) and at the end (b) of the drying process (140°C, vacuum) of injection molded potato starch.

means that starch molecules that do not belong to the network of double helices (peak 1) should be disordered single helices (peaks 2 and 3) connecting the net-point regions. To understand the structural changes occurring during vacuum drying of amorphous starch, it is sufficient to follow one of the two structural characteristics. Here, we have chosen the net-points of double helices.

From Figure 2, one can distinguish four characteristic regions during the drying process at 140°C, while at 120°C three of them coincide:

Region I. During the first 1–2 min, at both temperatures, a sudden increase of the double helix content is observed. Simultaneously, the spacing d_1 (peak 1) increases from 0.66 to 0.676 nm, a value that for longer
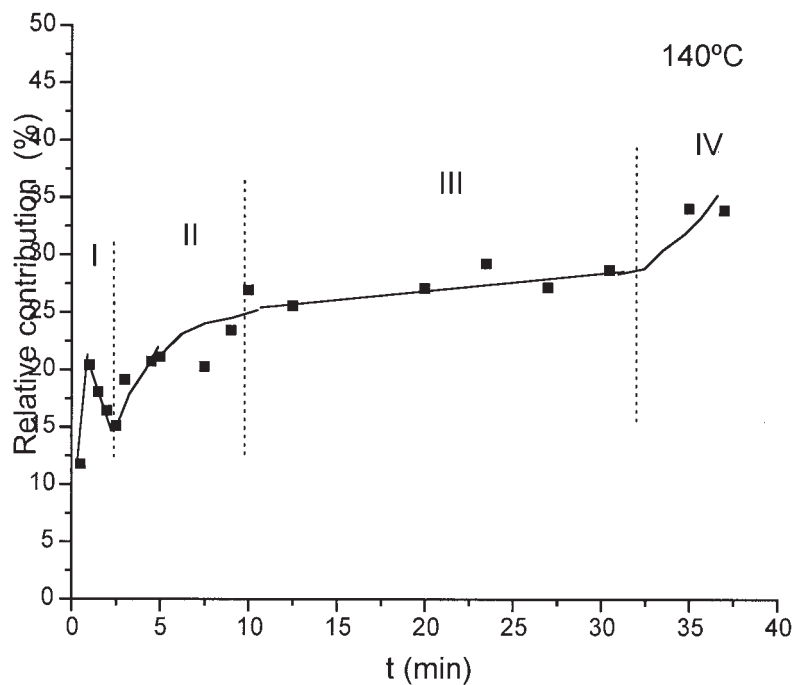
(a)
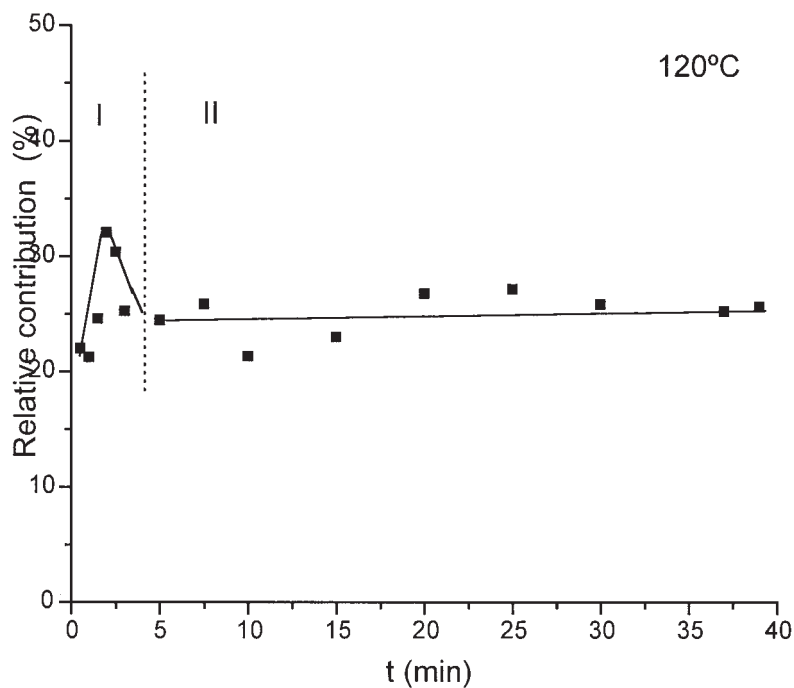
(b)

Figure 2 Relative contribution of the double helix component to the WAXS pattern, as a function of drying time: (a) 140°C drying temperature; (b) 120°C drying temperature.

times does not change anymore. This can be explained by the thermal expansion of the samples, initially held at room temperature, and then heated up on the sample holder. During this time, the initially room-atmo-

sphere conditioned sample begins to dry from the outer side within the heated vacuum. Because of the shrinkage of the sample, single helices tend to approach among themselves to form double helices. This

inhomogeneous drying leads to inner tensions as already mentioned in Bayer *et al.*[7] which cause an unraveling process of the double helices (decrease at the end of region I).

Region II. In case of heating at 140°C (Fig. 2(a)), an increase of double helices is observed up to a saturation value. Obviously, the increased inner mobility due to the loss of fixation of the primary network leads to an increase of double helix formation. The inner tensions created by the drying process are oriented towards the force bearing centers of the primary network. At 140°C, the entanglement network is not fixed anymore, chains may glide through the net-points. The forces applied to the starch molecules now act on the newly formed secondary double helix network, leading to an increase in formation of double helices. Apparently, both components of the starch network are not cooperative. The formation of the secondary double helix network can only take place if the primary network of entanglements does not hinder it (like at 120°C, Fig. 2(b)). Bernazzani[11] shows that the FTIR band of the amylose network is reinforced by an increase of the cooling velocity after subjecting the starch sample to a given annealing temperature T_a. The intensity band suddenly increases if T_a reaches the region of the melting of the fixed entanglement network (above 120°C), i.e., the hindrance to the formation of double helices is now reduced.

It is worth mentioning that the secondary network of double helices can develop during the drying process at such high temperatures. Starch–water gels, whose connecting zones are also referred to as double helices, dissolve at 70°C. The relation of peak 1 to water content is discussed later.

Regions III and IV. After all free water has been dried out, a saturation value of the double helix content is observed. Only in the case of 140°C, a further increase is observed (region IV) that might be due to an evaporation of water molecules, which are strongly bound to the starch molecules.[7]

Effect of water uptake in amorphous starch

The WAXS patterns in Figures 3(a)–(c) summarize the very complex structural changes that take place during the penetration of water into amorphous potato starch, while a time–temperature program is developed.
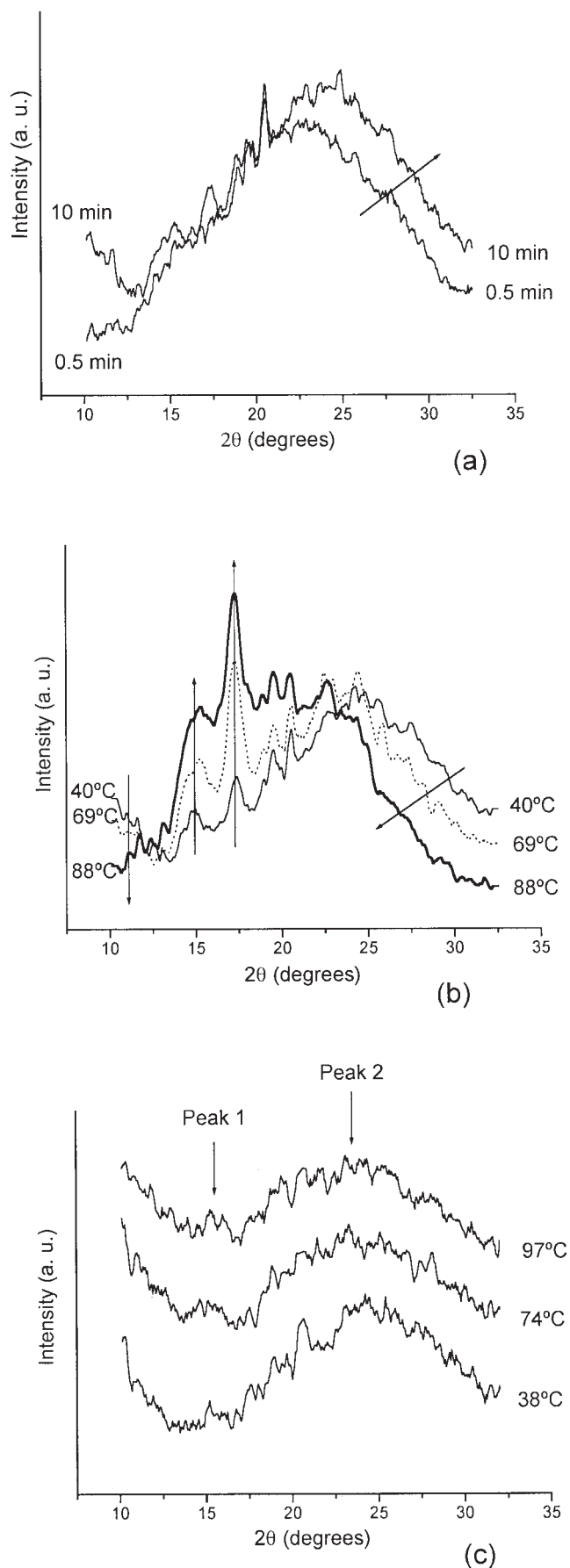

(a)

(b)

(c)

Figure 3 WAXS patterns of potato starch injection moldings under the influence of water- saturated air. (a) Room temperature: 0.5 and 10 min of exposure to humid air; (b) stepwise increase of temperature of the water-saturated air; (c) stepwise decrease of temperature from the molten state of water-saturated potato starch.

Figure 3(a) characterizes the structure changes at room temperature. The initial WAXS pattern differs somewhat from that in Figure 1(a). In spite of the fact that, in both cases, one starts from room atmosphere conditioned amorphous materials, the sample used in Figure 1(a) has been dried before the first X-ray diffraction run, while the sample used in Figures 3(a) and 3(b) has been subjected to a humid atmosphere before starting the experiment. Although the low angle region of the scattering pattern is not much affected, the high angle flank is considerably shifted to increasing scattering angles, giving rise to a shift of the maximum and an increment of its broadening. This is still more pronounced, when the water further diffuses into the sample during the next 10 min (Fig. 3(a)). The intensity of peak 1 has considerably diminished when compared with the drying process (Fig. 1). The double-helix regions, thus seem to be sensitive against water. When the temperature approaches 70°C, the double-helix regions should have fully disappeared (see Fig. 3(c)).

Because the scattering component describing the higher angular region of the WAXS pattern has been attributed to disordered single helices (peak 2), the influence of water might be interpreted as giving rise to a rapprochement of single helices.

The WAXS diagram obtained at 40°C (see Fig. 3(b)) indicates that the shift of the single helix peak stops, when the first crystalline reflections appear, i.e., at $2\theta_{300} \approx 17°$. A further increase of annealing temperature (Fig. 3(b)) shows the development of the crystalline peaks at expense of the broadening of the scattering pattern at higher angles (closer-packed single helices) (back-shift in Fig. 3(b)). The simultaneous development of the two phenomena suggests that a correlation exists. Figure 3(a) suggests the closer-packed single helices as precursors of double helices, which in a further step initiate crystallization. The area of the amorphous halo comprised between the two right flanks of Fig. 3a (related to the closer-packed single helices) disappears from the WAXS pattern and new maxima, corresponding to the double helix crystalline reflections, emerge.

Below $2\theta = 12.5°$, one sees the background development during water penetration. At room temperature, (Fig. 3(a)), this effect strongly increases and is maintained with increasing temperature up to 69°C, in contrast to the evolution of the right flank, which already shifts back at smaller angles at 40°C.

The intensity increase of the diffractogram in the background region because of water penetration could be explained by water molecules that act as spacers between starch molecules. Because of the increase in mean distances, scattering intensity increases at smaller scattering angles.[3] WAXS patterns of Delmas[10] show that the disappearance of the background at small scattering angles does not occur before the

(100) B-crystal reflection (not detected here) emerges. Since this process induces a long-range order of crystal water, it is delayed with respect to the formation of the first crystalline reflections (i.e., (300)). The background may be, hence, considered as precursor of the (100) reflection, i.e., after formation of the first crystals (f.e. 300–reflection) disordered water molecules from the background gradually transform into ordered crystal water (100–reflection). The background vanishes when (100) begins to emerge (WAXS pattern of Bernazzani et al. [10]). The disappearance of the background involves an improvement of the crystal structure, which has been built up under control of the secondary network (below 70°C). Not before the secondary network melts (above 70°C), the water molecules of the background arrange into crystal water, giving rise for the disappearance of the background (Fig. 3(b), $T = 88°C$). Simultaneously, water molecules that cannot be included into the crystal water arrangement are sweat out from the sample. At the end of the experiment, when the sample is finally cooled down to room temperature, one notices that water is removed from the crystallized gel.

The WAXS diffraction patterns from a wet melt at 97°C (Fig. 3(c)) reveal that no crystallization occurs, when it is cooled in steps from 72°C to 38°C. These diffraction patterns show that peak 2 exhibits the same broadening to higher scattering angles as observed for the water penetration in the molded amorphous starch at 25°C and 40°C (Figs. 3(a) and 3(b)). Only a slight modification of the WAXS pattern due to thermal expansion may be observed. A back-shift of the right flank of the WAXS pattern is not observed because crystallization does not take place. This appears to confirm indirectly the postulated relation between decreasing amount of neighboring single-helices (as a first step of crystallization) and the formation of double-helix crystals.

CONCLUSIONS

1. The X-ray scattering halo appearing in amorphous starch can be decomposed into three Gaussian components. The highest and lowest scattering angle maxima are associated with regions containing disordered single helices. The third (middle) component is associated to the scattering contribution of disordered regions from double helices. It is suggested that the disordered single helices form a three-dimensional network connected by a primary network of fixed amylose entanglements. Results show that during drying the number of double helices increases, which is considered as densification of the amylose network by a secondary network. It is suggested that the double helix peak corresponds to the secondary network alone.

2. The penetration of water has three effects: (a) a higher molecular mobility leading to a closer helical packing that becomes the precursor of a double helix crystal formation; (b) an increase of intermolecular distances leading to the appearance of an excess of background scattering at small angles; (c) a weakening of the secondary network. When at 70°C, the secondary network disappears, water molecules reorganize as crystal water within the B-crystal, giving rise for the disappearance of the background scattering.

References

1. Willenbücher, R. W. Ph.D. Thesis, No. 10136, ETH Zürich, 1993.
2. Rueda, D. R.; Bayer, R. K.; Cagiao, M. E.; Baltá-Calleja, F. J. Structure variation of starch in a sealed capillary studied by real-time X-ray-scattering, Annual Report; DESY: Hamburg, 2001.
3. Müller, J. J.; Gernat, G.; Schulz, W.; Müller, E. C.; Vorwerg, W.; Damaschun, G. Biopolymers 1995, 35, 271.
4. Imberty, A.; Perez, S. Biopolymers 1988, 27, 1205.
5. Gidley, M. J. Macromolecules 1989, 22, 351.
6. Zobel, H. F. In Developments in Carbohydrate Chemistry; Alexander, R. J., Ed.; American Association of Cereal Chemists: St. Paul, MN, 1994.
7. Bayer, R. K.; Lindemann, S.; Dunkel, M.; Cagiao, M. E.; Ania, F. J Macromol Sci Phys 2001, B40, 733.
8. Waigh, T. A.; Perry, P.; Riekel, C.; Gidley, M. J.; Donald, A. M. Macromolecules 1998, 31, 7980.
9. Waigh, T. A.; Gidley, M. J.; Komanshek, B. U.; Donald, A. M. Carbohydr Res 2000, 328, 165.
10. Bernazzani, P.; Chapados, C.; Delmas, G. J Polym Sci Part B: Polym Phys 2000, 38, 1662.
11. Bernazzani, P.; Chapados, C.; Delmas, G. Biopolymers 2001, 58, 305.
12. Mercier, C.; Charbonniere, R.; Gallant, D.; Guilbot, A. In Polysaccharides in Food; Blanshard, J. M. V.; Mitchell, J. R., Eds.; Butterworth: London, 1979; p 153.
13. Cagiao, M. E.; Bayer, R. K.; Rueda, D. R.; Baltá–Calleja, F. J. J Appl Polym Sci 2003, 88, 17.
14. Bayer, R. K.; Baltá-Calleja, F. J. J Macromol Sci Phys 2005, 344, 1.
15. Liu, Q.; Charlet, G.; Yelle, S.; Arul, J. Food Res Int 2002, 35, 397.
16. Bayer, R. K.; Zachmann, H. G.; Baltá-Calleja, F. J.; Umbach, H. Polym Eng Sci 1989, 29, 188.
17. Lopez Cabarcos, E.; Zachmann, H. G.; Bayer, R. K.; Baltá-Calleja, F. J. Polym Eng Sci 1989, 29, 193.